

A New Method of Assessing Lipid Mixtures by ^{31}P Magic-Angle Spinning NMR

Dror E. Warschawski,^{1,2} Alexandre A. Arnold,¹ and Isabelle Marcotte^{1,*}

¹Department of Chemistry, Université du Québec à Montréal, Montréal, Québec, Canada and ²UMR 7099, CNRS-Université Paris Diderot, Institut de Biologie Physico-Chimique, Paris, France

ABSTRACT A variety of lipids that differ by their chains and headgroups are found in biomembranes. In addition to studying the overall membrane phase, determination of the structure, dynamics, and headgroup conformation of individual lipids in the mixture would be of great interest. We have thus developed, to our knowledge, a new approach using solid-state ^{31}P NMR, magic-angle spinning, and chemical-shift anisotropy (CSA) recoupling, using an altered version of the recoupling of chemical shift anisotropy (ROCSA) pulse sequence, here penned PROCSA. The resulting two-dimensional spectra allowed the simultaneous measurement of the isotropic chemical shift and CSA of each lipid headgroup, thus providing a valuable measure of its dynamics and structure. PROCSA was applied to mixtures of phosphatidylethanolamine (PE) and phosphatidylglycerol (PG) in various relative proportions, to mimic bacterial membranes and assess the respective roles of lipids in shaping these bilayers. The results were interpreted in terms of membrane topology, lipid propensity to adopt various phases or conformations, and lipid-lipid miscibility. Our results showed that PG dictates the lipid behavior when present in a proportion of 20 mol % or more. A small proportion of PG is thus able to impose a bilayer structure to the hexagonal phase forming PE. We discuss the requirement for lipids, such as PE, to be able to adopt non-bilayer phases in a membrane.

INTRODUCTION

There are over 40,000 different lipids in the LIPID MAPS database (<http://www.lipidmaps.org>), which differ mainly by their chains and headgroups. Such a stable diversity during evolution must reflect a specific role for each one of them, and the scarcity of knowledge around it is puzzling. Out of many examples in nature, one that is striking is the lipid composition of bacterial inner membranes. Although the inner membrane of Gram-negative bacteria such as *Escherichia coli* is composed of 77% phosphatidylethanolamine (PE), 20% phosphatidylglycerol (PG), and 3% cardiolipin (CL) (1), the plasma membrane of Gram-positive bacteria such as *Bacillus subtilis* (*B. subtilis*) is composed of the same phospholipids, but with a reverse ratio of PE to PG lipids (18% PE, 78% PG, and 4% cardiolipin, according to Clejan et al. (2)), and *Staphylococcus aureus* contains no PE (3). The role of cardiolipin is fascinating and would deserve a study of its own (4), but the question we address here is the

respective roles of PE and PG and their inverted proportions in the two bacterial types.

PEs are zwitterionic amphiphiles, whereas PGs are negatively charged at pH >5 and more hydrated than PE. Another very important difference between PE and PG is their propensity to adopt different phases. Although PG is a “lamellar-phase” lipid, PE is known to transition from lamellar to inverse hexagonal phases depending on temperature. Detailed phase changes in lipid bilayers can be followed by measuring order-parameter variation in the hydrocarbon chains, using ^2H nuclear magnetic resonance (NMR) with labeled lipids, for example (5–7). However, lipid phases can also be quickly assessed without isotopic labeling, from static solid-state ^{31}P NMR spectra in natural-abundance membranes (8,9). In NMR, the chemical shift anisotropy (CSA) reports on the immediate electromagnetic environment of the nucleus and is averaged out by molecular motions. The CSA is characterized by three parameters: its width, also called anisotropy, its asymmetry, and the isotropic chemical shift, i.e., where the signal would appear if the anisotropy was averaged out, for example, by very fast molecular motion or magic-angle spinning (MAS) of the sample. Each lipid possesses a single phosphorus atom whose CSA reports on the inclination of the lipid headgroup

Submitted September 1, 2017, and accepted for publication January 22, 2018.

*Correspondence: marcotte.isabelle@uqam.ca

Editor: Francesca Marassi.

<https://doi.org/10.1016/j.bpj.2018.01.025>

© 2018 Biophysical Society.



with respect to the membrane plane and on the lipid phase (lamellar/hexagonal, gel/fluid), but not on interlamellar spacing, for example. Although the asymmetry parameter is null in the fluid phase, the CSA decreases when the lipid headgroup moves toward the membrane plane and when the fluidity increases, notably above the phase-transition temperature, which allows for the detection of phase changes. The isotropic chemical shift, on the other hand, is characteristic of the lipid headgroup (PE, PG, and CL) and is much less sensitive to the lipid phase. In the case of lipid mixtures, various lipid spectra will overlap and it may become difficult to disentangle the various phases and dynamics associated with each lipid.

Over the years, several solutions have been suggested, which are summarized in an article by Moran and Janes (10), who debate on the compromise that has to be made between broadband NMR, which provides phase information, and high-resolution fast MAS NMR, which enables lipid identification as well as an increase in sensitivity. Moran and Janes suggest a slow MAS method that is a good trade-off when there are few lipids in a mixture that are in similar proportions and in very different phases. Here, we propose a different approach through two-dimensional (2D) NMR under fast MAS using a recoupling strategy that benefits from both broadband and high-resolution NMR. Although our approach also requires that lipids have different isotropic chemical shifts, we are able to measure the CSA of lipids, the proportion of which is <10 mol % in the mixture, even if they are in a slightly different phase.

Recoupling experiments in solid-state NMR, often performed in 2D, aim at correlating nuclei in a high-resolution spectrum with a specific interaction experienced by each nucleus. These experiments have gained a reputation for measuring ^{13}C - ^{15}N dipolar couplings for each ^{13}C (11), hence providing valuable distance measurements in proteins for biomolecular structure determination. In the case of lipids, measurement of ^{13}C - ^1H dipolar couplings for each ^{13}C made it possible to determine acyl chain order profiles in naturally abundant samples (12–14). Here, we were interested in measuring the ^{31}P CSA for each ^{31}P , hence the phase, dynamics, or headgroup orientation of each lipid in a mixture. ^{13}C CSA recoupling experiments have been developed in the past 40 years, from the original $2\text{-}\pi$ pulse sequence by Alla et al. (15) to the use of R-symmetry sequences (16). Other experiments make use of slow spinning frequencies, switched spinning frequencies, or switched angle spinning, but in the case of ^{31}P CSA recoupling in lipids, the experiment can be simplified, because ^{31}P is an abundant and sensitive nucleus that does not require cross-polarization, and because its coupling to protons is weak and does not require high-power decoupling. To preserve the shape of the recoupled spectrum, we have opted for the recoupling of chemical shift anisotropy (ROCSA) sequence (17), adapted to ^{31}P NMR.

Using this modified ^{31}P ROCSA sequence, dubbed PROCSA, we were able to provide 2D NMR spectra of lipid mixtures where the phase, dynamics, or structure of each constituent is easily determined. This experiment can be performed with a standard MAS probe at a moderate spinning frequency, and a spectrum can be obtained in <1 h. We successfully applied PROCSA to mixtures of PE, PG, and CL, in which we determined the phase of each lipid. Despite the overwhelming presence of PE in bacterial membranes, we show here that membranes with similar compositions adopt a PG-like behavior. In light of these results, the role of PE should be reconsidered, and its presence may only be necessary for specific processes such as membrane endocytosis, which is essential for bacterial infection.

MATERIALS AND METHODS

Materials

Phospholipids 1-palmitoyl-2-oleoyl-*sn*-glycero-3-phosphoethanolamine (POPE), 1-palmitoyl-2-oleoyl-*sn*-glycero-3-phospho-1'-*rac*-glycerol (POPG), and 1,1',2,2'-tetra-9Z-octadecenoyl-cardiolipin (TOCL) were obtained from Avanti Polar Lipids (Alabaster, AL) and used without further purification. Tris(hydroxymethyl)aminomethane (Tris), sodium chloride (NaCl), EDTA, and deuterium oxide (D_2O) were purchased from Bioshop Canada (Burlington, Ontario, Canada), ACP Chemicals (Montreal, Quebec, Canada), Fisher Scientific (Fair Lawn, NJ), and CDN Isotopes (Pointe-Claire, Quebec, Canada), respectively.

Sample preparation

Single lipids were used directly as a powder. Lipid mixtures were dissolved in chloroform/methanol (3:1) and dried under a nitrogen stream. Residual organic solvent was removed by pumping overnight with a mechanical vacuum pump. Samples were then hydrated at 75% in weight with a physiologically relevant buffer (100 mM Tris, 100 mM NaCl, and 2 mM EDTA (pH 7)) in D_2O . Each lipid dispersion was vortexed and freeze-thawed three times (10 min at -20°C followed by 10 min at 40°C) before ~ 30 mg of the sample was transferred into a disposable Kel-F insert and placed inside a 4 mm rotor. Each lipid composition was tested at least twice.

Nuclear magnetic resonance

All NMR experiments were carried out on a solid-state Bruker Avance III-HD wide bore 400 MHz spectrometer (Bruker, Milton, Ontario, Canada) operating at a frequency of 162 MHz for phosphorus, with a double-resonance 4 mm MAS probe. Temperature was calibrated and corrected at each spinning speed, and the equilibration time was at least 15 min between temperature steps. All spectra were processed with the Bruker TopSpin 3.5 interface.

One-dimensional (1D) static ^{31}P spectra were obtained using a phase-cycled Hahn echo pulse sequence with continuous-wave proton decoupling at a radio-frequency field strength of 50 kHz. Each spectrum was acquired with 128 or 256 scans, a (90°) pulse length of 3 μs , an interpulse delay of 30–40 μs , a recycle delay of 3 s, an acquisition time of 26 ms, and a dwell time of 5 μs (spectral width of 100 kHz), for a total time of 7–13 min. Processing was performed with left shifting by two to four points to start acquisition exactly from the top of the echo, automatic baseline correction, and a line broadening of 50 Hz. All 1D MAS ^{31}P spectra were acquired at a 6 kHz spinning rate (ω_r) with a simple (90°) pulse with two-pulse phase-modulated proton decoupling at a field strength of 25 kHz. Each spectrum was

acquired in 3 min, with 64 scans, a (90°) pulse length of 3 μ s, a recycle delay of 3 s, an acquisition time of 82 ms, and a dwell time of 10 μ s (spectral width of 50 kHz). Processing was performed with no line broadening. Considering the good signal/noise ratio, the uncertainty of ^{31}P chemical-shift measurements is on the order of ± 0.05 ppm.

The 2D MAS ^{31}P spectra were acquired at 6 kHz spinning rate with a modified ROCSA pulse sequence, with no cross polarization, named PROCESA. Proton decoupling during the recoupling time was performed using a proton (180°) pulse length of 5 μ s in the middle of each rotor period and, during acquisition, with two-pulse phase modulation at a field strength of 25 kHz. Phosphorus (90°) pulse length was 3 μ s, whereas PROCESA recoupling pulses, based on Cn_n^1 symmetry composite pulses described in the original work (17,18), were applied at a field strength of $4.28 \times \omega_r$ (see Fig. S1). Spectra were acquired with eight scans for each of the 32 rows, and a recycle delay of 3 s, for a total time of 14 min. The spectral width in the indirect dimension is ω_r , but since the spectra are recoupled with a scaling factor of 0.272, the indirect dwell time was artificially set to $0.272/\omega_r$ to rescale the recoupled spectrum to the same width as the static spectrum. Processing was performed with automatic baseline correction and no line broadening.

The 1D static ^{31}P spectra and ^{31}P slices of 2D PROCESA spectra were fitted using Bruker's software Sola (Solid Lineshape Analysis; Bruker), using Haeberlen's convention that provides the anisotropy that is commonly found in the literature. Overlap between spectra and fits was generally >90%, except in cases where a central dip was apparent in the recoupled spectra. Such a dip is expected in the case of ROCSA with few recoupled points (17), but it does not affect the anisotropy value, and it reduces the overlap to ~85%. We estimate the precision given by the fitting procedure to be $\sim \pm 2$ ppm for the anisotropy value.

RESULTS

Single lipids

Although they have been studied extensively since the 1970s (for example, (19–21)), there is no available table listing the ^{31}P CSAs of lipids according to their headgroups, aliphatic chains, buffer, temperature, or other physicochemical parameters. We have therefore acquired 1D static ^{31}P NMR spectra of all three lipids studied here in the same buffer and at several temperatures (see Fig. S2), and measured the corresponding isotropic shifts (δ) and anisotropies (Δ) (Table 1).

Only the isotropic shift of PE was sensitive to temperature, an effect already noticed by Estrada et al. (22) in organic solvents. As expected, the asymmetry parameter was null in all fluid samples. It was nonzero only for PE

TABLE 1 ^{31}P Static CSA (Δ) (± 2 ppm) and MAS Isotropic Chemical Shift (δ) (± 0.05 ppm) Values for Lipids at Various Temperatures

Temperature	POPE		POPG		TOCL	
	Δ	δ	Δ	δ	Δ	δ
0°C	35 (0.4)	−0.1	25	0.8	20	0.5
30°C	28	0	23*	0.8	19	0.5
75°C	−13	0.1	21*	0.8	18*	0.5

All asymmetry parameters are null, except when indicated in parentheses. An asterisk indicates the presence of a small isotropic component in addition to the major fluid lamellar signal. Isotropic chemical shifts are referenced to phosphoric acid 85%.

samples at 0°C, where lipids were in the gel phase. All other samples presented here were in the fluid lamellar phase, except for an occasional small isotropic component and for PE at 75°C, which was expectedly in the reverse hexagonal phase, as revealed by the change of sign of the CSA. When present, the small isotropic components disappear at 0°C and are therefore the result of a “reversible” phenomenon, potentially the appearance of small patches of disordered lipids in the bilayer. A striking phenomenon is the strong variation of CSA with temperature for PE, compared to a relatively stable value for PG.

Under MAS at 6 kHz, the broad ^{31}P spectrum splits into a narrow and intense central resonance, flanked by small spinning sidebands. This central isotropic resonance chemical shift (δ) also varied depending on headgroup and temperature, but all three lipids studied here exhibited isotropic chemical-shift differences of at least 0.3 ppm and could therefore be resolved, even at the moderate field strength of 400 MHz used here (Table 1). Since we had noted before that ^1H - ^{31}P heteronuclear decoupling was unnecessary above an 8 kHz spinning rate (23), we applied moderate (25 kHz) decoupling while spinning at 6 kHz, which resulted in a virtually undetectable line narrowing.

Model membranes

Since the ^{31}P CSA of a single lipid varies significantly depending on the lipid headgroup, its immediate environment, and temperature, we monitored the CSA of three essential lipids in mixtures of various compositions. Unfortunately, when lipid anisotropies are close, or when one lipid is much less abundant than the others, their CSAs overlap, and individual CSAs become hard to extract. We therefore had to resort to ^{31}P CSA recoupling experiments under MAS since at 6 kHz, PE, PG, and CL turn into narrow, separated, and intense resonances whose intensities reflect their abundance in the sample.

Despite other possibilities for ^{31}P CSA recoupling, we have decided to adapt the ROCSA sequence (17) to ^{31}P NMR with the ^{31}P nutation frequency during the recoupling time set to be 4.28 times the spinning frequency. We removed the initial cross-polarization step and ^{15}N decoupling, and we replaced the high-power continuous-wave (CW) ^1H decoupling during the recoupling time with a low-power decoupling performed using a proton (180°) pulse in the middle of each rotor period, hence creating the PROCESA pulse sequence shown in Fig. S1. In the original ROCSA sequence, the spinning frequency, which determines the sampling rate and the spectral width in the indirect dimension, was mostly limited by the available power for the CW ^1H decoupling. In PROCESA, this limit is almost lifted by the absence of such decoupling.

In the particular case of lipids, the largest anisotropy is <50 ppm, and PROCESA can be performed at relatively modest spinning frequencies. With our 400 MHz spectrometer,

6 kHz was found to be a good compromise for lipids. At this rate, between 32 and 64 points are worth acquiring in the indirect dimension, and since eight scans are sufficient for a good signal/noise ratio, the whole 2D spectrum can be acquired in under half an hour. Since ^{31}P resonates within <2 ppm for all phospholipids, PROCSA can be performed using an on-resonance pulse, and the resulting 2D spectrum is not sheared. An additional important feature of PROCSA is the shape preservation of the recoupled spectrum, which allows the use of the same fitting software for the recoupled slices as employed for static spectra.

We have applied the PROCSA sequence to membranes mimicking *E. coli* (77% PE, 20% PG, and 3% CL) and *B. subtilis* (18% PE, 78% PG, and 4% CL) and obtained 2D ^{31}P - ^{31}P spectra at the same three temperatures. Model membranes composed of phospholipids only, such as the ones presented here, do not represent bacterial membranes as a whole, but they differ by their lipid headgroup composition, leaving all other parameters, such as lipid acyl chains and protein content, constant. Examples are shown in Figs. 1 and 2 for spectra recorded at 30°C . Slices were extracted at the isotropic chemical shift of each individual lipid, and broad traces were obtained for each lipid, reflecting the typical recoupled ^{31}P spectrum that the lipid would have exhibited if it were static and isolated. Such a trace was fitted to a static ^{31}P spectrum by optimizing only the CSA isotropic value, anisotropy, and asymmetry parameters, as well as overall line broadening and intensity. An example is shown in Fig. 3, with slices extracted from Fig. 1. Anisotropy and asymmetry parameters were easily determined for individual lipids in the mixtures and are reported in Table 2.

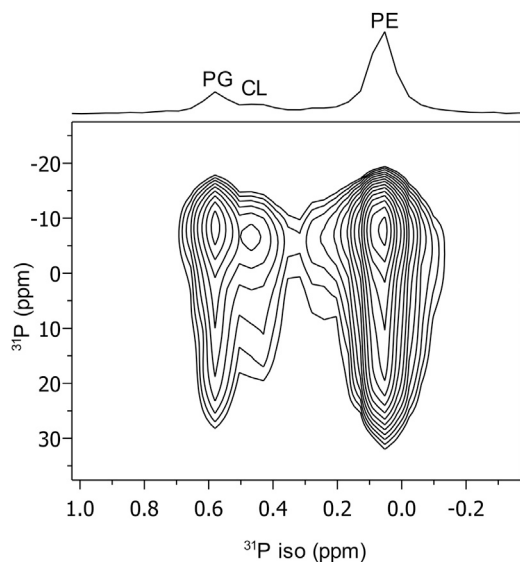


FIGURE 1 2D ^{31}P - ^{31}P PROCSA NMR spectrum of *E. coli* model membranes composed of 7 mg of POPE/POPG/TOCL 77:20:3 in $22\ \mu\text{L}$ of buffer at 30°C under MAS at 6 kHz (14 min acquisition). The projection is plotted to show the characteristic isotropic dimension.

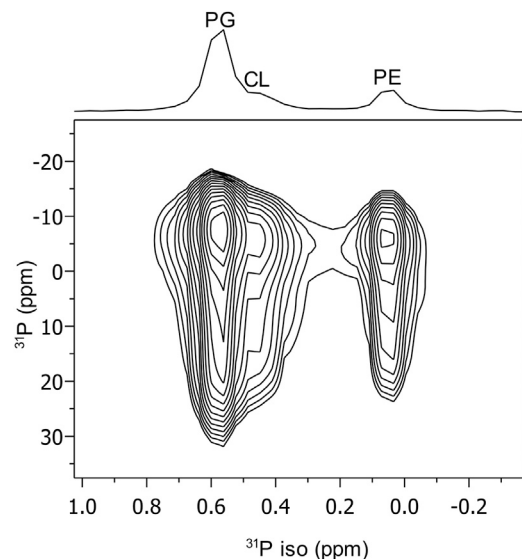


FIGURE 2 2D ^{31}P - ^{31}P PROCSA NMR spectrum of *B. subtilis* model membranes composed of 7 mg of POPE/POPG/TOCL 18:78:4 in $22\ \mu\text{L}$ of buffer at 30°C under MAS at 6 kHz (14 min acquisition). Note the changes in relative intensities in the isotropic dimension compared to the *E. coli* model membrane presented in Fig. 1.

In an ideal lipid mixture, individual lipids would be expected to adopt an average phase based on their relative proportions, and to some extent, this is what happens. When PG is the major lipid (*B. subtilis* model membrane), its CSA is the same as in pure PG membranes, whereas the anisotropy values of PE and CL tend to converge, in opposite directions, toward that of PG. Although the mixture remains in the fluid phase, this variation could result either from a change in dynamics, or from a change in lipid headgroup orientation. On the other hand, when PE is the major lipid (*E. coli* model membrane), it is only at 0°C —when the mixture is in the gel phase—that CSA values adopt an expected average value. Above 30°C , when the mixture is in the fluid phase, lipids tend to adopt a CSA reminiscent of that of PG alone instead of PE.

Two-lipid mixtures

Different lipid compositions affect various membrane properties (structure, dynamics, electrostatic interactions, packing, bending rigidity, etc.), which results in a ^{31}P CSA value that the experiment described in this article measures in a reliable fashion. To understand the role of PE versus PG in a bacterial membrane, we have simplified our model system even further by making samples of PE containing increasing proportions of PG. Our approach and findings are complementary to those obtained by Pozo Navas et al. (24), who followed phase changes using calorimetry, x-ray scattering, and microscopy in a very similar lipid-and-buffer model system. Those authors show that in such a system with varying ratios of PE to PG, the membrane organization

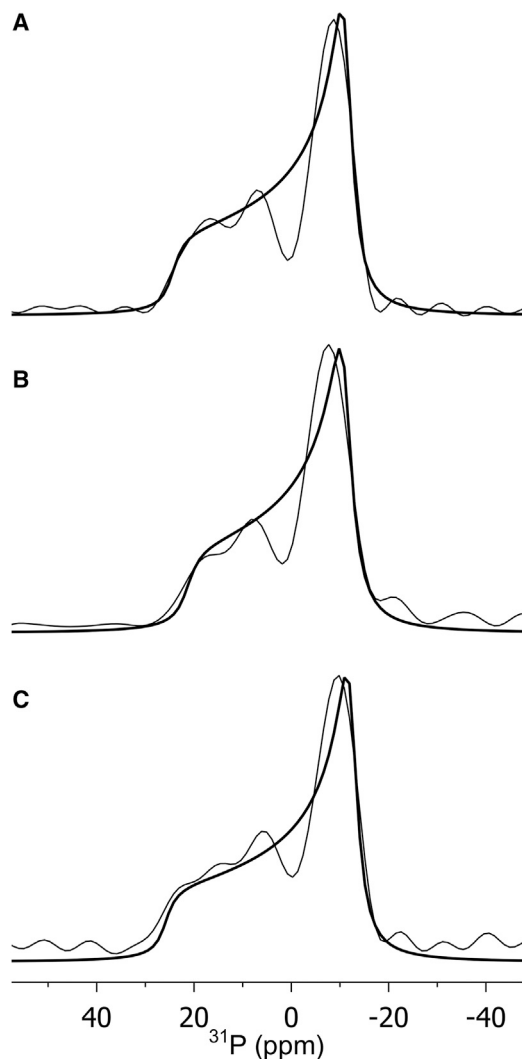


FIGURE 3 1D ^{31}P slices extracted from the 2D ^{31}P - ^{31}P PROCSA NMR spectrum of *E. coli* model membranes at 30°C (thin lines), superimposed with simulations using the software Sola (thick lines). Slices are taken at the isotropic chemical shifts of (A) PE, (B) CL, and (C) PG.

is dominated by interactions in the headgroup region rather than in the hydrocarbon chains. This is a strong incentive to use ^{31}P NMR as a complementary approach to ^2H NMR or other techniques.

Even at 50% PG, we were unable to distinguish two CSA patterns and assign them to PE and PG using 1D

TABLE 2 ^{31}P CSA Values (± 2 ppm) for Lipids in Model Membranes at Specific Temperatures

Model Membrane	POPE		POPG		TOCL	
	<i>E. coli</i>	<i>B. subtilis</i>	<i>E. coli</i>	<i>B. subtilis</i>	<i>E. coli</i>	<i>B. subtilis</i>
0°C	33 (0.4)	21 (0.2)	37 (0.5)	25 (0.2)	35 (0.5)	24 (0.2)
30°C	24	20	26	24	22	21
75°C	22	18	23	22	21	19

Values were determined by PROCSA NMR. All asymmetry parameters are null except when indicated between parentheses.

static ^{31}P NMR (see Fig. S3). On the other hand, the CSA values of PE and PG were readily measured in those samples by extraction from the PROCSA spectra at several temperatures, even in samples with only 10% of either lipid. The evolution of PE and PG CSA values with PG concentration is plotted in Fig. 4, and numerical values are reported in Table 3. To validate our approach, we first checked that the values extracted from the 2D PROCSA experiments on pure lipids corresponded to those measured on static 1D spectra. PROCSA resolution is indeed adequate for the determination of accurate anisotropy and asymmetry parameters, as can be seen by comparing the values extracted from the 2D spectra (Table 3) to the values measured in the 1D spectra (Table 1). Although PROCSA is thus capable of detecting phase changes, it is probably not sufficient to extract more detailed information such as lipid correlation or relaxation times. We could nevertheless ensure that the two-lipid systems behaved like the model membranes.

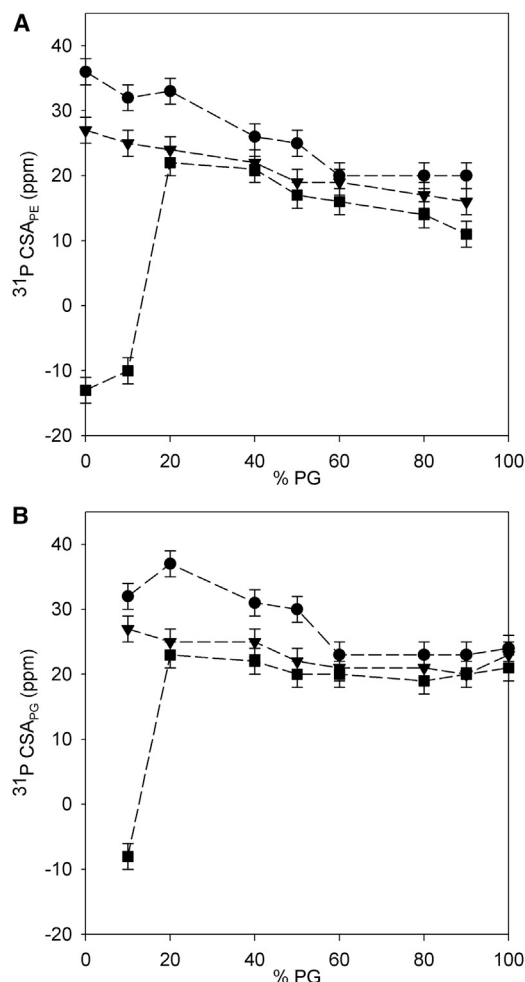


FIGURE 4 ^{31}P CSA anisotropy values (± 2 ppm) determined for PE (A) and PG (B) in their binary lipid mixtures at specific temperatures, as extracted from PROCSA experiments. Circles represent values at 0°C, triangles those at 30°C, and squares those at 75°C.

TABLE 3 ^{31}P Static CSA Values Determined for Individual Lipids in Lipid Mixtures at Specific Temperatures

	0°C		30°C		75°C	
	PE	PG	PE	PG	PE	PG
POPE	36 (0,4)		27		-13	
POPE/POPG:90/10	32 (0,4)	32 (0,4)	25	27	-10	-8
POPE/POPG:80/20	33 (0,4)	37 (0,3)	24	25	22	23
POPE/POPG:60/40	26 (0,3)	31 (0,3)	22	25	21	22
POPE/POPG:50/50	25 (0,3)	30 (0,2)	19	22	17	20
POPE/POPG:40/60	20 (0,1)	23 (0,1)	19	21	16	20
POPE/POPG:20/80	20 (0,2)	23 (0,2)	17	21	14	19
POPE/POPG:10/90	20 (0,3)	23 (0,2)	16	20	11	20
POPG		24		23		21

All values are given in ppm and were extracted from PROCESA experiments. Anisotropy values are determined ± 2 ppm. All asymmetry parameters are null except when indicated between parentheses.

With the addition of 10% PG, the mixture retains some of the properties of pure PE samples, for example, the existence of a hexagonal phase at high temperature and very broad lines in the gel phase. In the latter case, at 0°C, the resonance of PE is broad enough to hide that of PG, which can hardly be seen. However, in the fluid phase, addition of as little as 20% PG—a proportion encountered in *E. coli* membranes—was enough for the lipid CSA to be “dictated” by PG. Although the CSAs of PG in the mixtures were almost identical to that of pure PG (Fig. 4; Table 3), the CSA for PE in the mixture was reduced by the presence of PG. In addition, the hexagonal phase, present at 75°C in pure PE, disappeared in samples containing >20% PG. The only property that the mixture retained from PE, at all PG concentrations, was the presence of a gel phase at 0°C, with a slight, although reduced, asymmetry.

DISCUSSION

Lipid diversity in bacterial membranes has been discussed (25,26), with a particular emphasis on lipid chain diversity affecting membrane fluidity and hydrophobic mismatch to accommodate membrane proteins (6,7,27). Headgroup diversity has not been addressed as thoroughly, but it has been noted that the amount of nonlamellar lipids was also regulated (28–30) in bacterial membranes, and that discrimination between bacterial and mammalian cells by antimicrobial peptides was probably mainly due to the differences in lipid headgroup composition between the cell types (31). The approach presented here, using solid-state ^{31}P NMR and the 2D PROCESA sequence, may be able to fill this gap, by providing biologists with a simple tool to probe lipid headgroups and their physical state.

The PROCESA sequence is robust, easy to implement on a standard solid-state NMR equipment, and efficient in probing individual lipids in mixtures, even when they are <10% of the lipid population, provided that their resonance fre-

quency is resolved from other frequencies by ~ 0.1 ppm. The additional dimension increases the resolution and would allow an easy study of lipid CSAs in the presence of another phosphorus-containing molecule with a different chemical shift (free phosphate, for example), whereas it would interfere in a 1D spectrum. In this study, it was easy to resolve the headgroups of PE, CL, and PG. PROCESA can be used with very moderate decoupling power and at almost any rotor spinning frequency, depending on the available magnetic field. Finally, the simplicity of the PROCESA sequence enabled comparison of the resulting spectra to static and simulated spectra, using standard and commercial software.

The PROCESA sequence provides the ^{31}P CSA parameters of individual lipids in a mixture, which are generally related to the phase in which a lipid is found (e.g., hexagonal vs. lamellar for example), as well as its dynamics (e.g., gel versus fluid). As previously mentioned, the ^{31}P CSA is also affected by the inclination of the lipid polar headgroup relative to the membrane plane, which in turn can be affected by the membrane surface charge, notably conferred here by the negatively charged PG. The net charge of the membrane can be modified by the presence of charged molecules (32,33) or charged lipids (34). In this study, a combination of these contributions (electrostatic interactions, conformational changes, packing, and phase changes) may affect the CSA values measured by PROCESA and may explain their variations. Differentiating between those phenomena may be a difficult task and would require complementary experiments such as ^{14}N NMR to characterize the electrostatic membrane surface potential (34) and calorimetric measurements to detect phase changes (24,35). For example, in addition to the ability of PE to adopt a nonlamellar topology, it has been suggested to be a membrane stiffener (36), which would result in a decrease of the CSA with the addition of PG. However, the same effect could be explained by a tilt of its headgroup (as defined by the $\text{P}^-\text{-N}^+$ dipole), which would become more parallel to the membrane plane due to the increase in negative surface charges (34). Although the ^{31}P CSA in biomembranes results from a combination of many different membrane properties, as well as the roles potentially played by other lipids or membrane proteins, the results observed here inspire us to revisit the respective roles of PG and PE in a bacterial membrane.

In this study, we used PROCESA to measure the CSA of PE, PG, and CL lipids in mixtures mimicking Gram-positive and Gram-negative bacterial membranes, to hypothesize their roles in the cell membrane. In the absence of cholesterol, the introduction of PG in a PE bilayer is known to disrupt PE-PE contacts, to facilitate the formation of mixed pairs of PE-PG molecules and the hydration of PE headgroups, and to exhibit nonideal mixing properties (24,35). In addition, although cell membranes are generally structured as lipid bilayers in a lamellar phase, during fusion,

stalk formation, endocytosis, exocytosis, infection, division, and other processes, the bacterial membrane has to undergo various phase changes from lamellar to more complex hexagonal-like phases. Such transient and localized phases are believed to be present in biological membranes (37–39), and the experiments presented in this article might lend support to this hypothesis. Consequently, we were expecting to measure average CSA values, but we were also hoping to observe a particular role for PE, which gives the membrane its potential to adopt nonlamellar phases. Much to our surprise, none of these two scenarios occurred, and it seems that PG dictates the membrane phase, especially the native-like fluid lamellar phase, provided that it is at least 20 mol % abundant.

Unfortunately, the part played by the membrane in processes such as secretion, infection, or bacterial outer membrane vesicle entry into host cells has not been studied as much as that of the protein machinery (40). In such cases, PE is nevertheless thought to be able to better accommodate the membrane curvature frustration induced by these unusual structures (27,41). Our results suggest that this property of PE would not be exploited most of the time, and that it would become useful only when fusion, endocytosis, or other processes involving nonlamellar phases occurred that required demixing of PE from the membrane. Since PE has been reported to be much more abundant in Gram-negative bacteria, we hypothesize that these processes must be very different in Gram-positive bacteria, where the peptidoglycan might play a complementary part. Other hypotheses may exclude any structural role for PE and assume that its role is purely functional, since this lipid has been shown to be useful for the function of several membrane proteins, such as LacY, KcsA, and LmrP (25,26,42).

This article provides, to our knowledge, a new tool to help assess the role of lipids in biological processes, their structure, dynamics, and topologies, which have been somewhat neglected to date. After this initial study, we expect PROCESA to become widely applicable. Most commonly encountered phospholipids are easy to resolve by solid-state ^{31}P NMR: among PE, CL, PG, phosphatidylcholine, phosphatidylserine, and sphingomyelin, only PE and sphingomyelin would overlap. In the latter case, an additional dimension brought by the HOESY sequence may be a helpful improvement of the approach (23). Obvious applications of PROCESA would be the study of coexisting gel and fluid or hexagonal and lamellar phases, as well as the selective effect of ions or drugs on specific lipid headgroups (28,43).

In addition, thanks to its high sensitivity, PROCESA should be readily transposable to biological samples such as bacteria or eukaryotic cells, provided that they contain phospholipids, obvious candidates being red blood cells or mitochondria (39). If the ^{31}P resonances of the lipid headgroups are resolved, there is no doubt that their individual CSA values can be determined by the PROCESA approach. Whether the complex phase coexistence or changes

observed in model membranes will also be visible in biomembranes is an open question, the answer to which will also help to assign the respective roles of lipids and other membrane molecules in their collective physicochemical behavior.

CONCLUSIONS

The ^{31}P CSA is a very informative physicochemical parameter in the study of lipids in membranes, and PROCESA is, to our knowledge, a new and efficient 2D solid-state NMR approach to determine the CSA of individual lipids in complex lipid mixtures. It has allowed us to measure the ^{31}P CSA of three lipids in model membranes mimicking bacterial inner membranes. We have observed that PG dictates lipid behavior when present in a membrane in a proportion of 20 mol % or more. We hypothesize that PE is a “reserve” lipid that adapts to PG and changes phase only when necessary.

In-cell solid-state NMR is an emerging field that requires new tools to expand its range of applicability, and ^{31}P NMR is underrepresented as one of these tools (44,45). Recently, ^2H NMR has been adapted to in-cell and even in vivo solid-state NMR to characterize lipid acyl chains in intact bacterial membranes and examine the effect of antimicrobial peptides (6,7). The herein presented technique should enable measurement of complementary solid-state ^{31}P NMR spectra by assessing individual lipid headgroup conformations, or overall phases and rigidities, within a complex membrane environment.

SUPPORTING MATERIAL

Three figures are available at [http://www.biophysj.org/biophysj/supplemental/S0006-3495\(18\)30152-8](http://www.biophysj.org/biophysj/supplemental/S0006-3495(18)30152-8).

AUTHOR CONTRIBUTIONS

D.E.W., A.A.A., and I.M. designed the research and wrote the article. D.E.W. collected data. A.A.A. designed figures.

ACKNOWLEDGMENTS

This work was supported by the Centre National de la Recherche Scientifique (UMR 7099) and the Natural Sciences and Engineering Research Council of Canada (grant 326750-2013).

REFERENCES

1. Burnell, E., L. van Alphen, ..., B. de Kruijff. 1980. ^{31}P nuclear magnetic resonance and freeze-fracture electron microscopy studies on *Escherichia coli*. I. Cytoplasmic membrane and total phospholipids. *Biochim. Biophys. Acta.* 597:492–501.
2. Clejan, S., T. A. Krulwich, ..., D. Seto-Young. 1986. Membrane lipid composition of obligately and facultatively alkalophilic strains of *Bacillus* spp. *J. Bacteriol.* 168:334–340.

3. Hayami, M., A. Okabe, ..., Y. Kanemasa. 1979. Lipid composition of *Staphylococcus aureus* and its derived L-forms. *Microbiol. Immunol.* 23:435–442.
4. Lewis, R. N., and R. N. McElhane. 2009. The physicochemical properties of cardiolipin bilayers and cardiolipin-containing lipid membranes. *Biochim. Biophys. Acta.* 1788:2069–2079.
5. Davis, J. H. 1983. The description of membrane lipid conformation, order and dynamics by ^2H -NMR. *Biochim. Biophys. Acta.* 737:117–171.
6. Warnet, X. L., M. Laadhari, ..., D. E. Warschawski. 2016. A ^2H magic-angle spinning solid-state NMR characterisation of lipid membranes in intact bacteria. *Biochim. Biophys. Acta.* 1858:146–152.
7. Laadhari, M., A. A. Arnold, ..., I. Marcotte. 2016. Interaction of the antimicrobial peptides caerin 1.1 and aurein 1.2 with intact bacteria by ^2H solid-state NMR. *Biochim. Biophys. Acta.* 1858:2959–2964.
8. Seelig, J. 1978. ^{31}P nuclear magnetic resonance and the head group structure of phospholipids in membranes. *Biochim. Biophys. Acta.* 515:105–140.
9. Schiller, J., M. Müller, ..., D. Huster. 2007. ^{31}P NMR spectroscopy of phospholipids: from micelles to membranes. *Curr. Anal. Chem.* 3:283–301.
10. Moran, L., and N. Janes. 1998. Tracking phospholipid populations in polymorphism by sideband analyses of ^{31}P magic angle spinning NMR. *Biophys. J.* 75:867–879.
11. Gullion, T., and J. J. Schaefer. 1989. Rotational-echo double-resonance NMR. *J. Magn. Reson.* 81:196–200.
12. Gross, J. D., D. E. Warschawski, and R. G. Griffin. 1997. Dipolar recoupling in MAS NMR: a probe for segmental order in lipid bilayers. *J. Am. Chem. Soc.* 119:796–802.
13. Dvinskikh, S. V., V. Castro, and D. Sandström. 2005. Efficient solid-state NMR methods for measuring heteronuclear dipolar couplings in unoriented lipid membrane systems. *Phys. Chem. Chem. Phys.* 7:607–613.
14. Leftin, A., T. R. Molugu, ..., M. F. Brown. 2014. Area per lipid and cholesterol interactions in membranes from separated local-field ^{13}C NMR spectroscopy. *Biophys. J.* 107:2274–2286.
15. Alla, M. A., E. I. Kundla, and E. T. Lippmaa. 1978. Selective determination of anisotropic magnetic interactions from high-resolution NMR spectra of powdered samples. *JETP Lett.* 27:194–197.
16. Hou, G., I. J. Byeon, ..., T. Polenova. 2012. Recoupling of chemical shift anisotropy by R-symmetry sequences in magic angle spinning NMR spectroscopy. *J. Chem. Phys.* 137:134201.
17. Chan, J. C. C., and R. Tycko. 2003. Recoupling of chemical shift anisotropies in solid-state NMR under high-speed magic-angle spinning and in uniformly ^{13}C -labeled systems. *J. Chem. Phys.* 118:8378–8389.
18. Hohwy, M., H. J. Jakobsen, ..., N. C. Nielsen. 1998. Broadband dipolar recoupling in the nuclear magnetic resonance of rotating solids: a compensated C7 pulse sequence. *J. Chem. Phys.* 108:2686–2694.
19. Wohlgemuth, R., N. Waespe-Sarcevic, and J. Seelig. 1980. Bilayers of phosphatidylglycerol. A deuterium and phosphorus nuclear magnetic resonance study of the head-group region. *Biochemistry.* 19:3315–3321.
20. Marassi, F. M., and P. M. Macdonald. 1991. Response of the headgroup of phosphatidylglycerol to membrane surface charge as studied by deuterium and phosphorus-31 nuclear magnetic resonance. *Biochemistry.* 30:10558–10566.
21. Pinheiro, T. J., and A. Watts. 1994. Resolution of individual lipids in mixed phospholipid membranes and specific lipid-cytochrome c interactions by magic-angle spinning solid-state phosphorus-31 NMR. *Biochemistry.* 33:2459–2467.
22. Estrada, R., N. Stolowich, and M. C. Yappert. 2008. Influence of temperature on ^{31}P NMR chemical shifts of phospholipids and their metabolites I. In chloroform-methanol-water. *Anal. Biochem.* 380:41–50.
23. Warschawski, D. E., P. Fellmann, and P. F. Devaux. 1996. High resolution ^{31}P - ^1H two-dimensional Nuclear Magnetic Resonance spectra of unsaturated lipid mixtures spinning at the magic-angle. *Eur. Biophys. J.* 25:131–137.
24. Pozo Navas, B., K. Lohner, ..., G. Pabst. 2005. Composition dependence of vesicle morphology and mixing properties in a bacterial model membrane system. *Biochim. Biophys. Acta.* 1716:40–48.
25. Cronan, J. E. 2003. Bacterial membrane lipids: where do we stand? *Annu. Rev. Microbiol.* 57:203–224.
26. Grimard, V., M. Lensink, ..., C. Govaerts. 2014. The role of lipid composition on bacterial membrane protein conformation and function. In *Bacterial Membranes: Structural and Molecular Biology*. H. Remaut and R. Fronzes, eds. Caister Academic Press, pp. 195–224.
27. Holthuis, J. C., and A. K. Menon. 2014. Lipid landscapes and pipelines in membrane homeostasis. *Nature.* 510:48–57.
28. Rietveld, A. G., J. A. Killian, ..., B. de Kruijff. 1993. Polymorphic regulation of membrane phospholipid composition in *Escherichia coli*. *J. Biol. Chem.* 268:12427–12433.
29. Rietveld, A. G., M. C. Koorengel, and B. de Kruijff. 1995. Non-bilayer lipids are required for efficient protein transport across the plasma membrane of *Escherichia coli*. *EMBO J.* 14:5506–5513.
30. Morein, S., A. Andersson, ..., G. Lindblom. 1996. Wild-type *Escherichia coli* cells regulate the membrane lipid composition in a “window” between gel and non-lamellar structures. *J. Biol. Chem.* 271:6801–6809.
31. Lohner, K., and E. J. Prenner. 1999. Differential scanning calorimetry and x-ray diffraction studies of the specificity of the interaction of antimicrobial peptides with membrane-mimetic systems. *Biochim. Biophys. Acta.* 1462:141–156.
32. Scherer, P. G., and J. Seelig. 1989. Electric charge effects on phospholipid headgroups. Phosphatidylcholine in mixtures with cationic and anionic amphiphiles. *Biochemistry.* 28:7720–7728.
33. Bechinger, B., and J. Seelig. 1991. Interaction of electric dipoles with phospholipid head groups. A ^2H and ^{31}P NMR study of phloretin and phloretin analogues in phosphatidylcholine membranes. *Biochemistry.* 30:3923–3929.
34. Lindström, F., P. T. Williamson, and G. Gröbner. 2005. Molecular insight into the electrostatic membrane surface potential by $^{14}\text{N}/^{31}\text{P}$ MAS NMR spectroscopy: nociceptin-lipid association. *J. Am. Chem. Soc.* 127:6610–6616.
35. Garidel, P., and A. Blume. 2000. Miscibility of phosphatidylethanolamine-phosphatidylglycerol mixtures as a function of pH and acyl chain length. *Eur. Biophys. J.* 28:629–638.
36. Dawaliby, R., C. Trubbia, ..., C. Govaerts. 2016. Phosphatidylethanolamine is a key regulator of membrane fluidity in eukaryotic cells. *J. Biol. Chem.* 291:3658–3667.
37. Yorke, M. A., and D. H. Dickson. 1985. Lamellar to tubular conformational changes in the endoplasmic reticulum of the retinal pigment epithelium of the newt, *Notophthalmus viridescens*. *Cell Tissue Res.* 241:629–637.
38. Garab, G., B. Ughy, ..., P. H. Lambrev. 2017. Lipid polymorphism in chloroplast thylakoid membranes—as revealed by ^{31}P -NMR and time-resolved merocyanine fluorescence spectroscopy. *Sci. Rep.* 7:13343.
39. Gasanov, S. E., A. A. Kim, ..., R. K. Dagda. 2018. Non-bilayer structures in mitochondrial membranes regulate ATP synthase activity. *Biochim. Biophys. Acta.* 1860:586–599.
40. O’Donoghue, E. J., and A. M. Krachler. 2016. Mechanisms of outer membrane vesicle entry into host cells. *Cell. Microbiol.* 18:1508–1517.
41. Lee, A. G. 2004. How lipids affect the activities of integral membrane proteins. *Biochim. Biophys. Acta.* 1666:62–87.
42. Hakizimana, P., M. Masureel, ..., C. Govaerts. 2008. Interactions between phosphatidylethanolamine headgroup and LmrP, a multidrug

- transporter: a conserved mechanism for proton gradient sensing? *J. Biol. Chem.* 283:9369–9376.
43. Santos, J. S., D. K. Lee, and A. Ramamoorthy. 2004. Effects of antidepressants on the conformation of phospholipid headgroups studied by solid-state NMR. *Magn. Reson. Chem.* 42:105–114.
 44. Warnet, X. L., A. A. Arnold, ..., D. E. Warschawski. 2015. In-cell solid-state NMR: an emerging technique for the study of biological membranes. *Biophys. J.* 109:2461–2466.
 45. Kaur, H., A. Lakatos-Karoly, ..., C. Glaubitz. 2016. Coupled ATPase-adenylate kinase activity in ABC transporters. *Nat. Commun.* 7:13864.

Biophysical Journal, Volume 114

Supplemental Information

A New Method of Assessing Lipid Mixtures by ^{31}P Magic-Angle Spinning NMR

Dror E. Warschawski, Alexandre A. Arnold, and Isabelle Marcotte

Supporting Material for

A new method of assessing lipid mixtures

by ^{31}P Magic Angle Spinning NMR

Dror E. Warschawski, Alexandre A. Arnold and Isabelle Marcotte

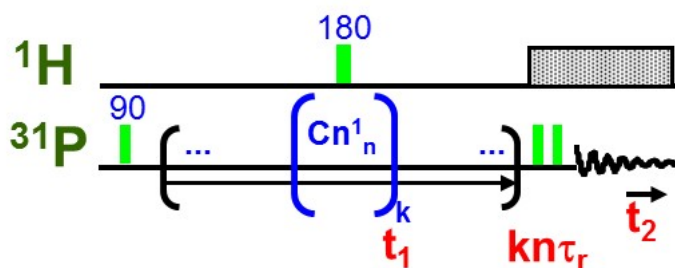


Figure S1. The PROCSA pulse sequence. Phosphorous excitation is performed by a simple (90°) pulse. Recoupling during t_1 is based on k cycles of C_n^1 composite pulses, with a phosphorous nutation frequency of $4.28 \times \omega_r$. Each C_n^1 spans n rotor periods ($n\tau_r$). The last two pulses make a z-filter, used to eliminate any residual transverse magnetization. Proton decoupling during t_1 is performed by a simple (180°) pulse in the middle of each rotor period. Proton decoupling during t_2 is performed by low-power TPPM.

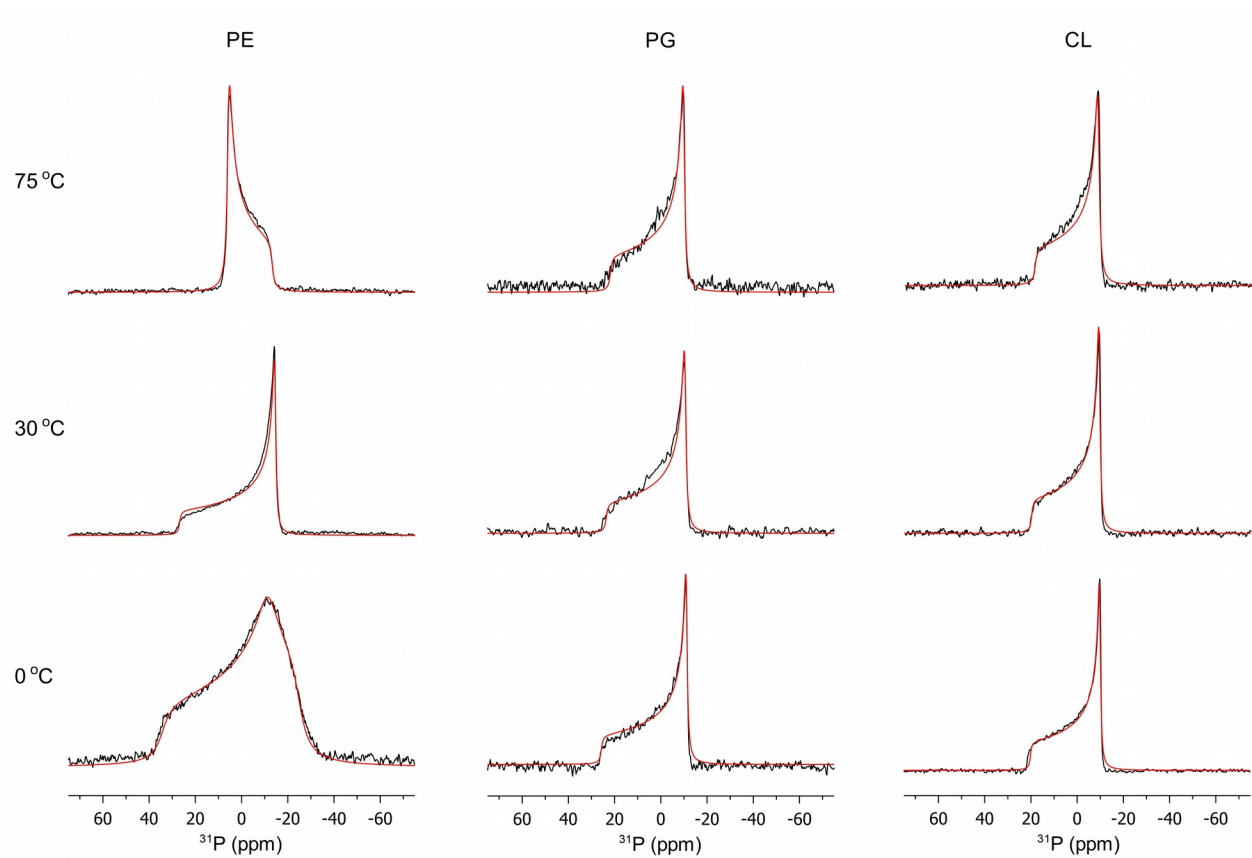


Figure S2. 1D static ^{31}P NMR spectra of individual lipids at several temperatures (black lines), superimposed with simulations using the software Sola (red lines). The extracted CSA values are reported on Table 1. As indicated, PE is on the left column, PG in the central column, and CL on the right column. The bottom line is at 0°C, the central line at 30°C, and the top line and 75°C.

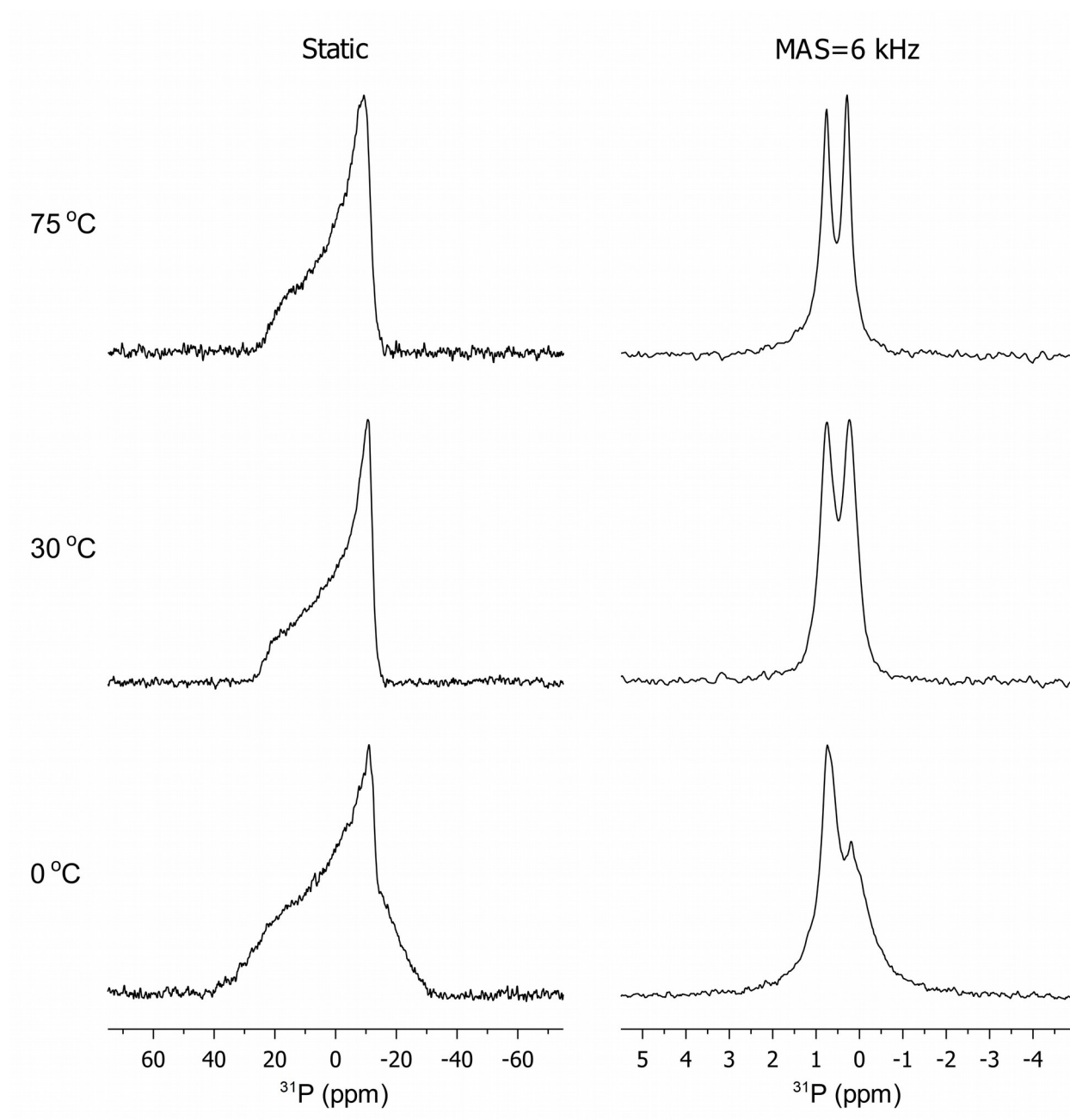


Figure S3. 1D ^{31}P NMR spectra of POPE/POPG:50/50. As indicated, the left column is for static samples and the right column is under MAS at 6 kHz. The bottom line is at 0°C , the central line at 30°C , and the top line and 75°C .